The Competition Between the Intramolecular Hydrogen Bond and pi-Electron Delocalization in Trifluoroacetylacetone-A Theoretical Study

ARTICLE *in* INTERNATIONAL JOURNAL OF QUANTUM CHEMISTRY · MARCH 2011

Impact Factor: 1.43 · DOI: 10.1002/qua.22129

4 AUTHORS, INCLUDING:

Alireza Nowroozi
University of Sistan and Baluchestan
37 PUBLICATIONS **312** CITATIONS
SEE PROFILE

Mohammad Sadegh Sadeghi
Ferdowsi University Of Mashhad
18 PUBLICATIONS **63** CITATIONS
SEE PROFILE

The Competition Between the Intramolecular Hydrogen Bond and π-Electron Delocalization in Trifluoroacetylacetone—A Theoretical Study

ALIREZA NOWROOZI, HOSSAIN ROOHI, MOHAMMAD SADEGH SADEGHI GHOOGHERI, MOHSENEH SHEIBANINIA

Department of Chemistry, Faculty of Science, University of Sistan and Baluchestan, P.O. Box 98135–674, Zahedan, Iran

Received 1 January 2009; accepted 16 January 2009
Published online 00 Month 2009 in Wiley InterScience (www.interscience.wiley.com).
DOI 10.1002/qua.22129

ABSTRACT: Conformational study of trifluoroacetylacetone was carried out using the HF, B3LYP, and MP2 methods with the 6-31G(d, p) and 6-311++G(d, p) basis sets. All of the results show that the chelated enol structures (E11 and E31) have extra stability with respect to the other forms and one of them (E11) is global minimum. The energy gap between the chelated forms is in the range 0.7–5.9 kJ mol^{-1}. Theoretical calculations show that this compound has an asymmetric double minimum potential energy surface which is in contrast with the electron diffraction result. Moreover, the computational results predict that due to the withdrawing effect of CF_3 group, hydrogen bond in trifluoroacetylacetone is weaker than the acetylacetone. Because of the more stability of E11, it is expected that the hydrogen bond energy in E11 is greater than the E31, but at all of the computational levels with most extended basis set the converse results were observed. These results clearly show that the hydrogen bond is not a superior parameter in conformational preference and the contribution of resonance is probably greater than the hydrogen bond. Finally, the analysis of this system by quantum theory of atoms in molecules and natural bond orbital methods fairly support the ab initio results. Int J Quantum Chem 000: 000–000, 2010

Correspondence to: A. Nowroozi; e-mail: anowroozi@chem.usb.ac.ir

Contract grant sponsor: Sistan and Baluchestan University (USB).

Key words: trifluoroacetylacetone; intramolecular hydrogen bond; ab initio; AIM; NBO

Introduction

β-dicarbonyl compounds display the keto=enol tautomerism with slow proton transfer and high concentration of enol tautomers in most cases. The chelated cis enol forms are stabilized by intramolecular hydrogen bond (IHB) and are predominant in the gas phase [1–3]. The most famous and simple members of these compounds are malonaldehyde and acetylacetone (AA) which have been extensively studied [4–8].

Trifluoroacetylacetone (TFAA) is unique among the AA derivatives so far investigated. This molecule is a simple fluorinated β-dicarbonyl that can be a model for the study of complex systems. TFAA has an asymmetric structure which lies between the AA and hexafluoroacetylacetone (HFAA) structures. We expect that the nature of the IHB, π-electron delocalization, and conformational composition of TFAA was extensively changed with respect to AA and HFAA. Thus, the comprehensive study of TFAA can give the significant information on the evolution of molecular properties on going from AA to TFAA and then HFAA. TFAA can participate in keto=enol tautomeric equilibrium with two different chelated enol forms, E11 and E31 (Fig. 1).

Although the X-ray crystal structure of TFAA was not investigated, but a symmetrical chelated ring with a linear hydrogen bond was reported by using the electron diffraction method [9]. Furthermore, semiempirical and ab initio studies were performed on TFAA with poor basis set that cannot produce a clear description of the system [10–12]. Recently, mechanism of UV-induced conformational changes among the enol types of TFAA were studied [13]. Finally, the various DFT levels and experimental FTIR and FT-Raman methods were used and a comprehensive vibrational analysis of this molecule was carried out [14]. Except these few studies, as far as we know, no further experimental and theoretical data about the structure of TFAA has been reported. By analyzing the published results about the structure of TFAA, we felt that it is necessary to carry out an extensive theoretical study of this compound. The main goal of the present study is prediction of the most stable structure among the plausible conformations and evaluation of the nature of IHB and π-electron delocalization in chelated forms. Furthermore, a detailed population analysis for some of the stable conformers of TFAA were performed by natural bond orbitals (NBO) [15] and atoms in molecules (AIM) [16] methods.

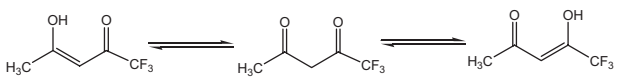

FIGURE 1. Tautomeric equilibriums in TFAA.

Method of Analysis

All of the computations in the present study were performed by Gaussian 98 series of programs [17]. The geometry optimizations were carried out by HF, B3LYP, and MP2 methods with 6-31G(d, p) basis set. Harmonic vibrational frequencies were calculated at these levels, except MP2, to confirm the nature of the stationary points found and evaluated the zero-point vibrational energy correction. The correct description of systems requires the inclusion of diffuse functions. Hence, we refine all of the computation with most extended basis set, 6-311++G(d, p).

The optimized structures at MP2/6-311++G(d, p) level were used to obtain the appropriate wave function files for AIM and NBO analyses. The nature of the IHB in the most stable forms have been studied by using the AIM theory of Bader by means of AIM2000 [18] software. Additionally, for better understanding the nature of IHB and conformational preference, the NBO analysis was performed by using the NBO package included in Gaussian program [19].

Results and Discussion

MOLECULAR CONFORMATION

Theoretical structure of all of the conformers are presented in Figure 2 and the optimized energies at HF, MP2, and B3LYP levels of theory are also given in Table I. According to the relative energies of HB enol, non-HB enol, and keto conformers at various ab initio levels, we can conclude the following energy order:

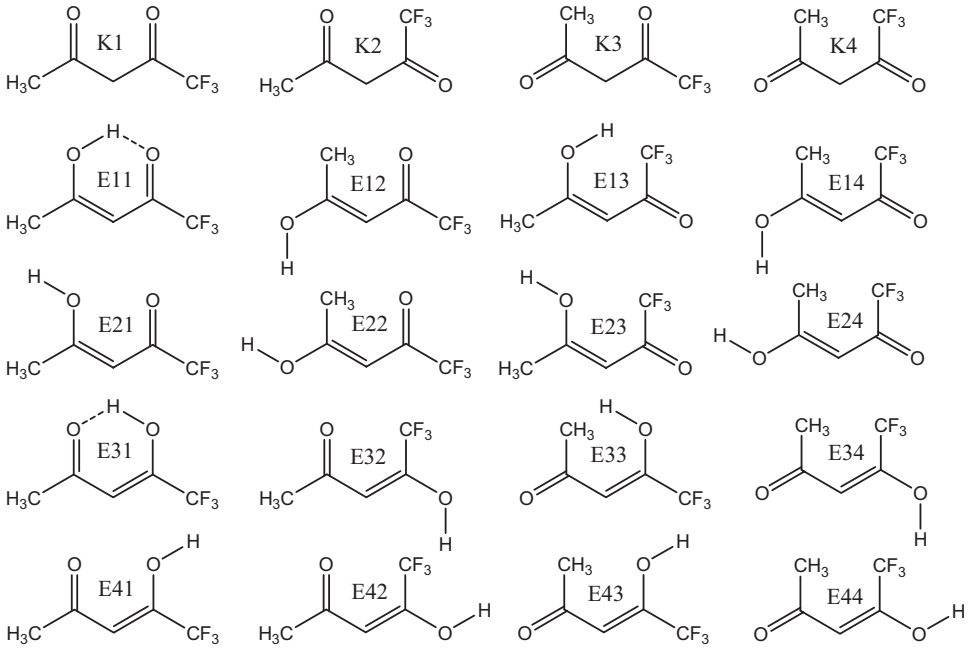

FIGURE 2. Theoretical structures of TFAA conformers.

$$\text{HB enol} < \text{keto} < \text{non-HB enol}$$

The energy gaps between these groups are readily assigned to the enolization process, IHB formation, and π-electron delocalization.

In the simple ketones, such as acetone, the enolization of keto functional group destabilized the molecule. From the mean values of bond energies [20], the destabilization energy due to the enolization process can be calculated, which is about 56.0 kJ mol^{-1}. The similar result is also obtained from the theoretical calculation at MP2/6–311++G(d, p) level of theory, which is about 64 kJ mol^{-1}. In non-HB enol forms of TFAA, the conjugation between the double bonds significantly decreases their energies. Therefore, the energy difference between the keto and non-HB enol groups is readily assigned to the π-electron delocalization and keto=enol tautomerism. Because of the extra stability of hydrogen bonded forms, the Boltzmann distribution function predicts that the presence of keto forms or non-HB enol forms in the conformational equilibrium are unlikely. Finally, from the relative energies, it can be concluded that this energy order is independent from the computational level and electron correlation energy. While, the energy gap between keto conformers and each of the enol groups strongly depend on the theoretical level and electron correlation.

The Keto Group

For TFAA four different planar diketo conformers (K1-K4) were considered. Full optimization of these forms at MP2 and B3LYP levels shows three local minimum on the potential energy surface (PES), which is named by Ka, Kb, and Kc. While, at HF level four local minimum were observed and belong to different enantiomer pairs. Our computational results exhibit that after full optimization, K1 and K3 forms are converted to the Ka, while K2 and K4 are converted to the Kb and Kc, respectively (Fig. 3). The absence of imaginary frequency for Ka, Kb, and Kc readily shows that these forms correspond to the true energy minima.

At MP2 level of theory, Kb has smaller energy which increased to Ka and Kc, while at B3LYP level Ka is more stable than the others. Consequently, the energy order in keto forms depend on the theoretical level and basis sets size. Since, the MP2/6-311++G(d, p) results are more reliable than the other levels, therefore, we accepted the following energy order:

$$\text{Kb} < \text{Ka} < \text{Kc}$$

It is firstly expected that the more stability of Kb is related to the C—H···O═C interaction, but in AIM molecular graph, no bond critical point (BCP)

TABLE I

Relative energies of TFAA conformers (kJ mol^{-1}).

	Method					
	B3LYP		MP2		HF	
Conformer	a	b	a	b	a	b
E11	0.0	0.0	0.0	0.0	0.0	0.0
E12	43.2	37.4	39.1	36.7	32.5	30.4
E13	48.6	48.2	45.3	44.8	45.8	45.6
E14	62.9	59.0	58.4	54.3	57.8	54.8
E21	62.8	54.0	57.3	50.3	51.4	46.7
E22	48.6	42.2	45.5	42.2	40.4	37.6
E23	68.7	61.1	63.1	55.0	56.9	52.2
E24	72.0	66.4	68.1	62.2	69.2	64.9
E31	4.4	5.9	0.70	2.2	1.9	2.9
E32	77.8	77.3	69.3	68.1	66.7	67.9
E33	63.0	58.2	54.8	50.5	52.4	49.2
E34	79.1	77.7	72.0	68.5	72.0	67.6
E41	64.4	61.1	57.2	54.6	54.6	52.2
E42	65.6	66.9	59.5	60.4	59.4	61.6
E43	57.6	53.4	49.0	45.6	45.4	42.4
E44	75.5	75.5	70.7	67.9	71.1	67.1
K1(Ka)	36.9	34.6	15.8	17.9	9.0	7.1
K2(Kb)	38.7	36.0	14.1	16.0	9.0	7.1
K3(Ka)	36.9	34.6	15.8	17.9	9.2	6.9
K4(Kc)	37.3	34.9	15.6	18.2	9.2	6.9

a: With 6–31G(d, p) basis set, b: with 6–311.

between these fragments was observed. Contrary to expectation, the existence of additional BCPs in Ka and Kc emphasize on the formation of C—H···O═C bond (Fig. 4). The values of ρ_{BCP} and $\nabla^2\rho_{BCP}$ at these BCPs, are about 0.00896 and −0.00827 (Ka), 0.00838 and −0.00759 a.u (Kc), respectively, which suggest the presence of weak interaction.

In the absence of any strong stabilizing factor, it seems that the small energy difference between Kb, Ka, and Kc is related to the dipole–dipole interaction. From the carbonyls arrangement, we can conclude that the repulsive interactions in Ka and Kc are probably greater than the Kb and the later has more stability with respect to the others.

The Enol Group

All of the enol conformers were fully optimized by using the HF, MP2, and B3LYP methods with the most popular basis sets, 6-31G(d, p) and 6-311++G(d, p), and their energies are given in Table I. The absence of imaginary frequency proved

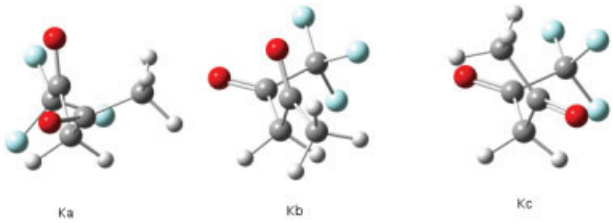

FIGURE 3. The optimized structures of keto forms at MP2/6-311++G (d, p) level of theory. [Color figure can be viewed in the online issue, which is available at www.interscience.wiley.com.]

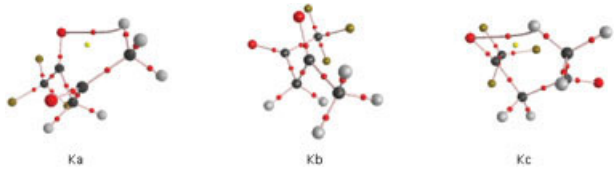

FIGURE 4. Molecular graph of keto forms at MP2/6-311++G (d, p) level of theory. [Color figure can be viewed in the online issue, which is available at www.interscience.wiley.com.]

that all of these planar forms have a particular local minimum on PES and all of them are stable.

The optimized energy at all of the computational levels show that the most stable (E11, E31) and least stable (E34, E32) pairs have significant energy difference with respect to the other forms. The energies of other forms are close together and their order strongly depends on the computational level. The theoretical calculations show that at all of the levels, except HF/6-311++G (d, p), E34 is the most unstable conformer. Furthermore, at all of the levels E11 is the most stable form or global minimum, that followed by E31, but the energy gap between them (ΔE) is in the range of 0.7–5.9 kJ mol^{-1}. Finally, we can assign the energy gap between the E11 and E31 to the IHB and π-electron delocalization energies. In the other parts of this work we focused on these items.

TABLE II

The Shuster hydrogen bond energy of chelated forms (kJ mol^{-1}).

	AA	E11	E31	HFAA
MP2				
6-31G(d, p)	67.94	57.33	56.44	45.08
6-311++G(d, p)	61.85	50.34	52.36	40.36
B3LYP				
6-31G(d, p)	72.84	62.77	59.95	48.53
6-311++G(d, p)	66.38	54.01	55.18	42.47
HF				
6-31G(d, p)	63.09	51.43	52.73	41.26
6-311++G(d, p)	58.90	46.70	49.33	37.40

HYDROGEN BOND

The extra stability of chelated forms is mainly due to the formation of IHB, which is assisted by π-electron delocalization (RAHB). Gilli and coworkers [21–26] have proposed the RAHB model as linking the strength of the hydrogen bond to the resonance in chelated systems. The IHB energy plays a significant role in conformational preference and its value strongly depends on the choice of the reference state. Many authors [27–31] have devised various methods to estimate the energy of IHB. In Shuster method, it is assumed that the energy difference between the close (with HB) and open (without HB) conformers to be equal with IHB energy. Finally, the resultant IHB energy contains some conformational contributions and its value is overestimated.

In this work, we also calculated the hydrogen bond energy by the Shuster method [27] and the results are given in Table II. It is evident from this table that at all of the computational levels, except MP2/6-31G(d, p) and B3LYP/6-31G(d, p), the Shuster hydrogen bond energy of E31 is greater than the E11. The greater value of Shuster HB energy in E31 with respect to E11 can be readily assigned to electron withdrawing effects of CF_3 group.

AIM Analysis

The AIM is a very useful tool in analyzing the hydrogen bond. The formation of HB is associated with the appearance of a BCP between the hydrogen atom of donor group and acceptor atom. Popelier and Bader [32] proposed a set of criteria for the existence of hydrogen bonding within the AIM formalism. Two criteria are connected with electron density, ρ_{BCP}, and its Laplacian, $\nabla^2\rho_{BCP}$, at BCP of hydrogen bonded systems and the others are related to the integrated properties of the H atom. The range of ρ_{BCP} and $\nabla^2\rho_{BCP}$ for normal HB are 0.002–0.035 and 0.024–0.139 a.u., respectively.

The topological parameters (ρ_{BCP}, $\nabla^2\rho_{BCP}$) of all of the chelated ring BCPs of E11, E31, AA, and HFAA are evaluated at MP2/6-311++G(d, p) level and the results are given in Table III. In all of the HB critical points, the values of ρ_{BCP} and $\nabla^2\rho_{BCP}$ are in the range 0.04155–0.05307 and 0.03726–0.04203 a.u., respectively. These characteristic of electron densities and its Laplacian at BCPs signify the presence of HB interaction. It can also be observed that the electron density and its Laplacian at the O···H BCP decreases from AA to E31, E11, and then HFAA.

Comparison between the topological properties of E11and E31 shows that these values for E31 are slightly greater than the corresponding value of E11. Hence, the HB in E31 is slightly stronger than the E11. In the same manner, we can conclude that the IHB in AA is stronger than the E31 and the HB in HFAA is weaker than the E11. Therefore, the HB energy obeys from the following order:

$$E_{HB}(HFAA) < E_{HB}(E11) < E_{HB}(E31) < E_{HB}(AA)$$

This conclusion is strongly supported by hydrogen bond energies. Finally, the results of Table III shows that for all of the system studied here, the value of charge density and its Laplacian are located in the

TABLE III

Topological parameters of BCPs in chelated rings (a.u.).

	ρ_{BCP}				$\nabla^2\rho_{BCP}$			
Bond	E11	E31	AA	HFAA	E11	E31	AA	HFAA
O···H	0.04661	0.05066	0.05307	0.04155	−0.03990	−0.04090	−0.04203	−0.03726
O—H	0.32892	0.32069	0.32130	0.33162	0.61682	0.59856	0.59661	0.62634
C═O	0.38915	0.38472	0.38169	0.39308	0.02709	0.01793	0.027642	0.00961
C—C	0.29979	0.29141	0.29516	0.29575	0.22916	0.22015	0.22291	0.22605
C═C	0.32811	0.33153	0.32969	0.33088	0.26007	0.26084	0.26100	0.26020
C—O	0.31707	0.32243	0.31458	0.32317	0.04903	0.06975	0.05503	0.06282

above-mentioned range. It means that these systems belong to the strong IHBs.

NBO Analysis

The formation of hydrogen bond implies that a certain amount of electronic charge is transferred from the proton acceptor to the proton donor and a rearrangement of electron density within each part of the molecule occurred. In the NBO analysis, the electronic wave functions are interpreted in terms of a set of occupied Lewis and a set of non Lewis localized orbitals [33]. Electron delocalization or charge transfer effects can be identified from the presence of off diagonal elements of the Fock matrix in the NBO basis. The strengths of these delocalization interactions, $E^{(2)}$, are estimated by second-order perturbation theory.

In Table IV, the NBO occupation numbers for the σ^*(O—H) antibonds, the oxygen lone pairs (n_O), and their respective orbital energies (ε) are reported. Furthermore, some significant donor-acceptor interactions and their second-order perturbation stabilization energies $E^{(2)}$ at the MP2/6-311++G(d, p) level for chelated forms of TFAA, HFAA, and AA are also given. In NBO analysis of HB systems, the charge transfer between the lone pairs of proton acceptor and antibonds of proton donor is most significant. As we know, the HB charge transfer greatly change the occupation number of oxygen lone pairs and σ^*(O—H). The occupation number of σ^*(O—H) in non HB conformers is very small, while the corresponding value for oxygen lone pairs is very close to the standard value of 2. These values explicitly show that no charge transfer between the lone pair of carbonyl oxygen and σ^*(O—H) occurred. The corresponding values in chelated conformers are greatly changed. The occu-

TABLE IV

The selective NBO results at MP2/6-311++G (d, p) level of theory.

	E11	E31	E21	E41
$Lp \rightarrow \sigma^*_{OH}$	28.30	33.51	0.000	0.00
$O.N\sigma^*_{OH}$	0.0455	0.0514	0.0068	0.0070
$O.N_{Lp}$	1.89239	1.89832	1.90522	1.91748
E (Lp)	−0.51374	−0.53465	−0.45823	−0.44823
E (σ_{*OH})	0.6325	0.6215	0.6391	0.6396
	AA1	AA2	HFAA1	HFAA2
$Lp \rightarrow \sigma^*_{OH}$	36.11	0.00	22.90	0.00
$O.N\sigma^*_{OH}$	0.0550	0.0067	0.0383	0.0070
$O.N_{Lp}$	1.89541	1.91826	1.89770	1.90520
E (Lp)	−0.50709	−0.41878	−0.54065	−0.48913
E (σ_{*OH})	0.6530	0.6610	0.6062	0.6177

$E_{Lp \rightarrow \sigma^*OH}$ (in kcal mol^{-1}).
$E_{Orbital}$ (in a.u.).

TABLE V
Structural parameters of chelated forms (Å).

	E11	E31
$r_{(C—O)}$	1.326	1.323
$r_{(C═C)}$	1.376	1.363
$r_{(C—C)}$	1.434	1.461
$r_{(C═O)}$	1.240	1.243
$q_1 = r_{(C—O)} - r_{(C═O)}$	0.086	0.080
$q_2 = r_{(C—C)} - r_{(C═C)}$	0.058	0.098
$Q = q_1 + q_2$	0.144	0.178

pation number of the σ^*(O—H) antibonds increases from HFAA to E11, E31, and AA, and their orbital energies are also increasing in the same manner. These results can be rationalized in terms of the charge transfer interaction between orbitals. As a consequence, the similar trend is predicted for IHB strength, which is consistent with the AIM analysis and Shuster hydrogen bond energy values.

As illustrated in Table IV, the results of NBO analysis show that in chelated structures of HFAA, E11, E31, and AA conformers, two lone pairs of oxygen atom participate as donor and the σ^*(O—H) antibonds as acceptor in strong intramolecular charge transfer interaction with stabilization energy value of 22.90, 28.30, 33.51, and 36.11 kcal mol^{-1}, respectively. Similarly, we can observe that the charge transfer energy increases on going from HFAA to E11, E31, and then AA. This order again supports the previous results about the IHB strength in chelated forms of HFAA, TFAA, and AA.

RESONANCE

The π-electron delocalization is a very well-known phenomenon that exist in simple and complex molecules and influences the chemical reactivity and chemical reactions [34, 35]. The influence of π-electron delocalization on the characteristic of HB is also introduced. It has been shown that in RAHB systems, the IHB and π-electron delocalization are coupled. This phenomenon changed the geometrical structure, geometrical parameters, and vibrational frequencies.

Although, E11 and E31 have similar structures but the HB energy of E31 is greater than the corresponding value of E11 and one may probably imagine that the E31 is the most stable form. Unlike expectation, all of the theoretical calculations emphasize on E11 as the most stable form. This duality clearly shows that the IHB energy can not determine the global minimum and π-electron delocalization can be probably solving this problem as a superior factor.

Resonance tends to decrease the single bond length and increase the double bond length. Thus from the Gillis parameters, q_1, q_2, and Q, we can estimate the greatness of resonance, qualitatively. The bond length and the value of q_1, q_2, and Q parameters for E11 and E31 are also given in Table V. These results reveal that the π-electron delocalization of E11 is greater than the E31. The value of q_1 for E11 and E31 are near equal, but q_2 and Q in these forms are significantly differing. For instance, the value of Q for E11 and E31 are about 0.144 and 0.178 Å, respectively.

The existence of π-electron delocalization implies that a certain amount of electronic charge is transferred and a rearrangement of electron density occurred. These electronic charge transfers are well estimated by NBO approach by second-order perturbation theory and are given in Table VI. The total values of charge transfer energies for E11 and E31 are about 169.6 and 144.4 kcal mol^{-1}, respectively. These results show that the π-electron delocalization in E11 is very greater than the E31. It is obvious from this table, the greatness of resonance in E11 respect with E31 is strongly related to the difference in charge transfer between the $\pi_{C═C}$ and $\pi^*_{C═O}$. It seems that, this difference is mainly due to the inductive effect of CF_3 group which is located near the C═C bond. Finally, the result of NBO analysis proves that the π-electron delocalization is only superior factor which determine the global minimum.

Conclusion

HF, MP2, and B3LYP theoretical methods are employed to optimize all of the TFAA conformers

TABLE VI
Some of the important charge transfer in chelated ring (kcal/mol).

Donor	Acceptor	E11	E31
n_{O2}	$\pi^*_{C═C}$	73.01	67.13
$\pi_{C═C}$	$\pi^*_{C═O}$	65.02	39.96
n_{O1}	σ^*_{OH}	28.30	33.51
$\pi_{C═O}$	$\pi^*_{C═C}$	3.29	3.79
Total		169.62	144.39

with the most popular basis sets. The NBO and AIM analyses were used to discuss the origin of conformational preference and the nature of IHB strength. Some conclusions may be drawn from the theoretical calculations:

According to the results, TFAA have 19 stable forms and therefore 19 local minimum.

- As expected, the chelated enol forms have greater stability with respect to the other forms and all of the computational levels emphasized on E11 as global minimum.
- The energy difference between the chelated forms (E11, E31) depends upon the choice of theoretical level and increase by enlargement of the size of the basis sets.
- Theoretical calculations show that the hydrogen bond strength increases from HFAA to AA (HFAA < E11 < E31 < AA). Topological analyses results also predict the similar order which is well supported by NBO results.
- A detailed population analysis of chelated forms (E11, E31) explicitly show that the origin of conformational preference is mainly due to the π-electron delocalization, especially the charge transfer between the $\pi_{C=C}$ and $\pi^*_{C=O}$.

References

1. Emsley, J. Structure and Bonding, Vol. 2; Springer: Berlin, 1984.
2. Jeffrey, G. A. An Introduction to Hydrogen Bonding; Oxford University Press: New York, 1997.
3. Grabowski, S. J. Hydrogen Bonding—New Insights; Springer: Berlin, 2006.
4. Woodford, J. N. J Phys Chem 2007, 111A, 8519.
5. Musin, R. N.; Mariam, Y. H. J Phys Org Chem 2006, 19, 425.
6. Boese, R.; Antipin, M. Y.; Blaser, D.; Lyssenko, K. A. J Phys Chem 1998, 102B, 8654.
7. Iijima, K.; Ohnogi, A.; Shibata, S. J Mol Struct 1987, 156, 111.
8. Rios, M. A.; Rodrigoes, J. J Mol Struct (THEOCHEM) 1990, 204, 137.
9. Anderssen, A. L.; Zebelman, D.; Baure, S. H. J Am Chem Soc 1971, 93, 1148.
10. Gordon, M. G.; Kobo, R. D. J Am Chem Soc 1993, 95, 5863.
11. Buemi, G. J Mol Struct (THEOCHEM) 2000, 499, 21.
12. Sliznev, V. V.; Lapshina, S. B.; Girichev, G. V. J Struct Chem 2006, 47, 220.
13. Minura, Y.; Nagashima, N.; Kudoh, S.; Nakata, M. J Phys Chem 2004, 108A, 2353.
14. Raissi, H.; Nowroozi, A.; Roozbeh, M.; Farzad, F. J Mol Struct 2006, 787, 148.
15. Reed, A. E.; Curtis, L. A.; Weinhold, F. A. Chem Rev 1988, 88, 899.
16. Bader, R. F. W. Atoms in Molecules. A Quantum Theory; Clarendon: Oxford, UK, 1990.
17. Frisch, M. J.; Trucks, G. W.; Schlegel, H. B.; Scuseria, G. E.; Robb, M. A.; Cheeseman, J. R.; Zakrzewski, V. G.; Montgomery, J. A. Jr.; Stratmann, R. E.; Burant, J. C.; Dapprich, S.; Millam, J. M.; Daniels, A. D.; Kudin, K. N.; Strain, M. C.; Farkas, O.; Tomasi, J.; Barone, V.; Cossi, M.; Cammi, R.; Mennucci, B.; Pomelli, C.; Adamo, C.; Clifford, S.; Ochterski, J.; Petersson, G. A.; Ayala, P. Y.; Cui, Q.; Morokuma, K.; Malick, D. K.; Rabuck, A. D.; Raghavachari, K.; Foresman, J. B.; Cioslowski, J.; Ortiz, J. V.; Baboul, A. G.; Stefanov, B. B.; Liu, G.; Liashenko, A.; Piskorz, P.; Komaromi, I.; Gomperts, R.; Martin, R. L.; Fox, D. J.; Keith, T.; Al-Laham, M. A.; Peng, C. Y.; Nanayakkara, A.; Gonzalez, C.; Challacombe, M.; Gill, P. M. W.; Johnson, B.; Chen, W.; Wong, M. W.; Andres, J. L.; Gonzalez, C.; Head-Gordon, M.; Replogle, E. S.; Pople, J. A. Gaussian 98, Revision A. 7; Gaussian, Inc: Pittsburgh, PA, 1998.
18. Biegler-König, F.; Schönbohm, J.; Bayles, D. J Comput Chem 2001, 22, 545.
19. Glendening, D. E.; Reed, A. E.; Carpenter, J. E.; Weinhold, F. NBO, Version 3.1; University of Wisconsin: Madison.
20. Pauling, L. The Nature of Chemical Bonds; Cornell University Press: New York, 1960.
21. Gilli, P.; Belluchi, F.; Ferretti, V.; Bertolasi, V. J Am Chem Soc 1989, 111, 1023.
22. Bertolasi, V.; Gilli, P.; Ferretti, V.; Gilli, G. J Am Chem Soc 1991, 113, 4917.
23. Gilli, P.; Bertolasi, V.; Ferretti, V.; Gilli, G. J Am Chem Soc 1994, 116, 909.
24. Gilli, P.; Bertolasi, V.; Ferretti, V.; Gilli, G. J Am Chem Soc 2000, 122, 10405.
25. Gilli, P.; Bertolasi, V.; Ferretti, V.; Gilli, G. J Am Chem Soc 2002, 124, 13554.
26. Gilli, P.; Bertolasi, V.; Ferretti, V.; Gilli, G. J Am Chem Soc 2004, 126, 3845.
27. Shuster, P.; Zundel, G. The Hydrogen Bond. Recent Development in Theory and Experiment; North Holland: Amsterdam, 1976.
28. Rozas, I.; Alkorta, I.; Elguero, J. J Phys Chem 2001, 105A, 10462.
29. Espinosa, E.; Molins, E. J Chem Phys 2000, 113, 5686.
30. Nowroozi, A.; Raissi, H.; Farzad, F. J Mol Struct (THEOCHEM) 2005, 730, 161.
31. Jablonski, M.; Kaczmarek, A.; Sadlej, A. J. J Phys Chem 2006, 110A, 10890.
32. Popelier, P. L. A.; Bader, R. F. W. J Phys Chem 1992, 189, 542.
33. Schleyer, P. V. R. Chem Rev 2005, 105, 3433.
34. Krygowski, T. M.; Cyranski, M. Chem Rev 2001, 101, 1385.
35. Grabowski, S. J. J Phys Org Chem 2003, 16, 797.